Structural transformation, amorphization, and fracture in nanowires: A multimillion-atom molecular dynamics study

Phillip Walsh, Wei Li, Rajiv K. Kalia, Aiichiro Nakano, and Priya Vashishta[a]
Concurrent Computing Laboratory for Materials Simulations and Biological Computation and Visualization Center, Department of Physics and Astronomy and Department of Computer Science, Louisiana State University, Baton Rouge, Louisiana 70803-4001

Subhash Saini
Numerical Aerospace Simulation Facility, NASA-Ames Research Center, Moffett Field, California 94035

Multimillion-atom molecular dynamics simulations of silicon diselenide nanowires are used to study mechanical properties and changes in nanowire structure under strain. The nanowires transform from a body-centered orthorhombic structure to a body-centered tetragonal structure under uniaxial strain, which causes an unexpected elongation in one of the transverse directions. For larger strains, the nanowires undergo a process of local amorphization, followed by fracture at one of the resulting crystalline–amorphous interfaces. The critical strain for fracture is 15%. Local temperature and stress distributions after failure are interpreted in terms of the local amorphization. © *2001 American Institute of Physics.* [DOI: 10.1063/1.1374237]

The study of mechanical properties and failure of nanowires is becoming an increasingly important area of materials science. Carbon nanotubes, as well as nanowires formed from other materials, are currently being investigated for their possible use as reinforcing fibers in high-strength/light-weight composite materials.[1] Self-assembling protein nanotubes may eventually be used for molecular electronics applications and in novel drug-delivery systems.[2] Stress-engineered gallium arsenide striped mesas and quantum dots are the basis for nanoscale optoelectronic devices.[3]

Silicon diselenide ($SiSe_2$) provides an interesting opportunity for nanowire research. It has a one-dimensional chain-like structure composed of exclusively edge-sharing tetrahedral units, so that a nanowire is easily constructed by simply removing a well-defined number of these chains from the bulk crystal. $SiSe_2$ nanowires have not yet been produced, though it is an active area of research. Recently, 1 μm long crystalline selenium nanowires with 60 nm diameters were experimentally produced.[4]

Crystalline $SiSe_2$ is orthorhombic with lattice constants $a = 9.669$ Å, $b = 5.998$ Å, and $c = 5.851$ Å, with four $SiSe_2$ tetrahedra per unit cell (see Fig. 1). The chain axis is along the bulk c axis. In this letter, we report simulations of $SiSe_2$ nanowires having circular cross sections, one having 128 chains and an initial length of 895 Å, and another having 1204 chains and an initial length of 3580 Å. The wires' diameters are 65 and 210 Å, respectively. We have characterized the nanowires' mechanical properties under strain and have observed an interesting strain-induced structural transformation. We have also characterized a process of local amorphization and fracture using local temperature and pressure profiles at critical strain. Previous simulations of $SiSe_2$ nanowires used smaller wires with rectangular cross sectional shapes.[5]

The interatomic potential used to characterize $SiSe_2$ contains two-body steric repulsion, screened Coulomb, and charge–dipole interactions. Covalent bonding effects are described by three-body bond angle terms. The potential gives good results for structural correlations and thermodynamic properties of $SiSe_2$ such as the calculated melting temperature and static structure factor.[5]

The 128-chain wire consisted of 117 504 total atoms, while the 1204-chain nanowire contained 4 465 152 atoms. The nanowires were relaxed for 3000 time steps at 0.01 K and again at 10 K before gradually heating to 100 K over 5000 time steps. The wires were then thermalized for 30 000 time steps. A MD time step of 1.5 fs was used throughout. Periodic boundary conditions were used in the c direction. The wires' cross sectional shapes changed slightly during the relaxation, so that the effective lattice constants became $a \approx 10.4$ Å and $b \approx 5.86$ Å. This was a result of the large surface area of the nanowires. After the thermalization, tensile strain was applied to the wires by uniformly scaling the atomic coordinates along the c axis in increments of 1%. Each extension was followed by a 3000 time step thermalization.

A structural transformation took place under strain. The peaks in the Si–Si pair distribution function corresponding to the lattice parameters ($a = 9.669$ Å and $b = 5.998$ Å) merged into one peak by 15% strain, corresponding to the new effective lattice constants, $a \approx b \approx 7.2$ Å (Fig. 2). This is essentially a shift from orthorhombic to tetragonal structure. The resulting cross sectional shape is shown in Fig. 1. The overall cross sectional shape changed from circular to elliptical, with the somewhat remarkable result that the wire expanded in one of the transverse directions. With the strain rate used in these simulations, the structural transformation happened gradually over several values of strain. In other words, the transformation is sluggish in comparison to the current strain rate. Simulations using a much slower strain rate are needed in order to determine the precise strain at which the transformation occurs. The structural transformation is currently be-
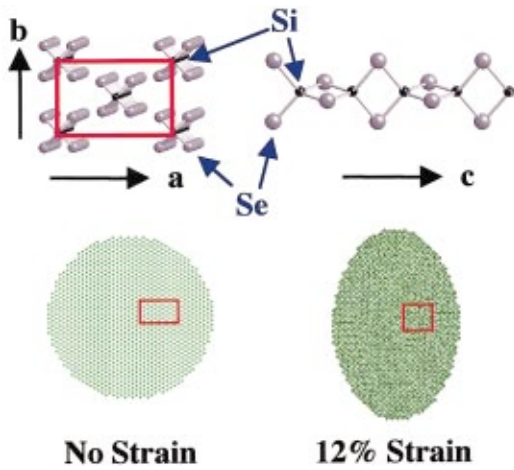
[a]Electronic mail: priyav@bit.csc.lsu.edu

FIG. 1. (Color) Top: schematic of SiSe₂ crystalline structure, showing the unit cell in the $a-b$ plane and the edge-sharing chain structure in the c direction. Bottom: cross sections of the 1204-chain wire at 0% strain (bottom left) and at 12% strain (bottom right). The nanowire extended in one transverse direction while contracting in the other so that the initially circular cross sectional shape became elliptic. The red boxes illustrate the change in the underlying lattice structure under strain.

ing studied in more detail using bulk SiSe₂ as well as additional nanowire simulations.

The nanowires remained crystalline and elastic up to 15% strain. The virial stress was used to derive a tensile stress versus strain curve for both wires, and a Young's modulus of ~130 GPa was obtained from the slopes of those curves.

At 15% strain, one of the Si–Se tetrahedral bonds in an outer chain broke and the undercoordinated silicon atom bonded with a selenium atom belonging to a neighboring chain in a corner-sharing configuration. This caused another Si–Se bond in the neighboring chain to break, setting off a chain reaction of this process throughout the transverse axis of the nanowire. The structure of amorphous SiSe₂ is known to consist of edge-sharing chain fragments cross linked to each other by corner-sharing tetrahedral units, which is thought to occur during melting due to the interaction of chain ends.[6] These simulations show how a similar amor-
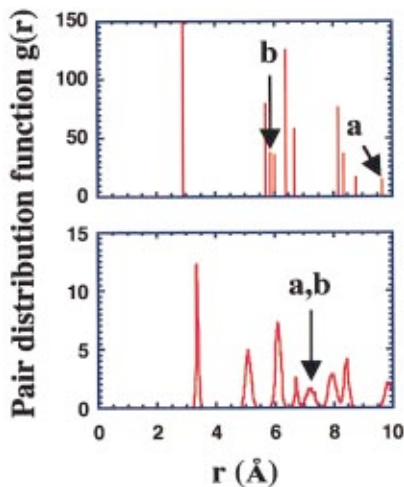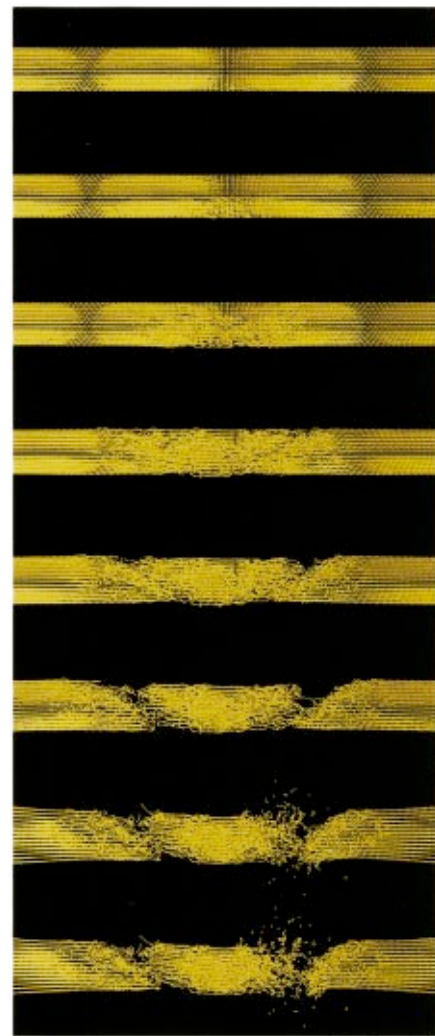

FIG. 3. (Color) Time progression of the atomic configuration for the 128-chain nanowire after reaching critical strain. Only the silicon atoms are shown.

FIG. 2. (Color) Si–Si pair distribution function for 0 K crystalline nanowire (top) and 100 K nanowire at 15% strain (bottom). Shifts in the a and b lattice parameters under strain are indicated.

FIG. 4. (Color) (a) Time progression of local tensile stress of the 1204-chain nanowire; (b) time progression of local kinetic temperature of the 1204 chain nanowire.

phization process can occur under the application of uniaxial strain.

The relationship between solid-state and quench-melt amorphization is still under debate. Experimental observations of solid-state amorphization include silicon,[7–9] germanium,[9] α-quartz,[10] and berlinite.[11] Solid-state amorphization has been studied in MD simulations of α-quartz[12] and berlinite.[13] Okamoto *et al.* have developed a unified conceptual framework for heat-induced melting and solid-state amorphization.[14] The selenium nanowires recently fabricated developed amorphous regions when exposed to radiation.[4]

Figure 3 shows the change in atomic configurations of the silicon atoms in the 128-chain nanowire with time at 15% strain. The disordered region is clear in contrast to the ordered chains of the crystal. The amorphization branches out in two directions. The result is a largely crystalline central section that is separated from the rest of the wire by the amorphous regions. Individual chains break on each side of this central region until only a few chains remain intact. These final chains break on one side, completely fracturing the wire.

The fracture process is similar in the 1204-chain nanowire, but local statistical quantities can be shown with much greater resolution due to the larger size. The local stress distribution was obtained by dividing the wire into $10 \times 10 \times 10$ Å^3 cells and computing the virial from the atoms in each cell. The local kinetic temperature was calculated similarly from the sum of the particles' kinetic energies in each cell. Figure 4(a) shows the local stress distribution after critical strain is reached. Most of the wire is stable at 18–20 GPa tensile stress. At ~1.5 ps after reaching 15% strain, the stress abruptly drops in a small outer section of the wire. This region spreads rapidly and by 27 ps there is a distinct central region where the tensile stress has vanished. This region is almost completely cut off from the rest of the wire. Figure 4(b) shows the corresponding spikes in the temperature distribution. The temperature spikes are associated with the recoil caused by broken edge-sharing bonds, and may therefore be used to follow the progression of the local amorphization. There are two main branches of amorphization, which form the two crystalline–amorphous interfaces. Multiple secondary branches of amorphization are also visible, but are contained between the two main branches. As in the case of 128-chain wire, there is no well-defined crack front. Rather, individual chain ends snap on either side of the central region, with the final fracture occurring at one crystalline–amorphous interface. A similar phenomenon—crack propagation preceded by melting—has been observed in intermetallic compounds and alloys.[15–17]

In summary, multimillion-atom MD simulations of 128- and 1204-chain SiSe$_2$ nanowires with circular cross sections were performed in order to study structural characteristics under strain and the dynamics of strain-induced amorphization and fracture. The SiSe$_2$ unit cell transformed from a body-centered orthorhombic structure to a body-centered tetragonal structure under strain, so that the overall cross sectional shape of the wires became elliptical. A Young's modulus of 130 GPa was obtained from the stress–strain relationship for both wires. The wires remained crystalline and elastic up to 15% strain, after which atomic configurations, local stress distributions, and local temperature distributions were used to characterize the development of amorphous regions with time. There was no well-defined crack front. Local stress distributions after critical strain show that a central region nearly became separated from the rest of the wire before final fracture took place. Finally, the branching patterns in the amorphization were revealed through the local temperature distributions.

[1] D. Srivastava, F. Dzegilenko, S. Barnard, S. Saini, M. Menon, and S. Weeratunga, in *Handbook of Nanostructured Materials and Nanotechnology*, edited by H. S. Nalwa (Academic, New York, 2000) Vol. 2, p. 665.

[2] M. R. Ghadiri, J. R. Granja, and L. K. Buehler, Nature (London) **369**, 301 (1994); M. R. Ghadiri, J. R. Granja, R. A. Milligan, D. E. McRee, and N. Khazanovich, *ibid.* **366**, 324 (1993).

[3] A. Konkar, A. Madhukar, and P. Chen, Appl. Phys. Lett. **72**, 220 (1998).

[4] A. Abdelouas, W. L. Gong, W. Lutze, J. A. Shelnutt, R. Franco, and I. Moura, Chem. Mater. **12**, 1510 (2000).

[5] W. Li, R. K. Kalia, and P. Vashishta, Phys. Rev. Lett. **77**, 2241 (1996).

[6] J. E. Griffiths, M. Malyj, G. P. Espinosa, and J. P. Remeika, Phys. Rev. B **30**, 6978 (1984).

[7] G. M. Pharr, W. C. Oliver, and D. R. Clarke, Scr. Metall. **23**, 1949 (1989).

[8] G. M. Pharr, W. C. Oliver, and D. S. Harding, J. Mater. Res. **6**, 1129 (1991).

[9] D. R. Clarke, M. C. Kroll, P. D. Kirchner, and R. F. Coof, Phys. Rev. Lett. **60**, 2156 (1988).

[10] L. E. McNeil and M. Grimsditch, Phys. Rev. Lett. **68**, 83 (1992).

[11] M. B. Kruger and R. Jeanloz, Science **249**, 647 (1990).

[12] R. M. Wentzcovitch, C. da Silva, J. R. Chelikowsky, and N. Binggeli, Phys. Rev. Lett. **80**, 2149 (1998).

[13] J. S. Tse and D. D. Klug, Science **255**, 1559 (1992).

[14] P. R. Okamoto, N. Q. Lam, and L. E. Rehn, Solid State Phys. **52**, 1 (1999).

[15] P. R. Okamoto, J. K. Heuer, N. Q. Lam, S. Ohnuki, Y. Matsukawa, K. Tozawa, and J. F. Stubbins, Appl. Phys. Lett. **73**, 473 (1998).

[16] J. K. Heuer, P. R. Okamoto, N. Q. Lam, and J. F. Stubbins, Appl. Phys. Lett. **76**, 3403 (2000).

[17] R. M. Lynden-Bell, J. Phys.: Condens. Matter **7**, 4603 (1995).